Energy & Buildings 170 (2018) 145–156

Contents lists available at ScienceDirect

Energy & Buildings

journal homepage: www.elsevier.com/locate/enbuild

Study on optimizing design of solar chimney for natural ventilation and smoke exhaustion

Xudong Cheng[a,*], Long Shi[b,*], Peng Dai[a], Guomin Zhang[b], Hui Yang[a], Jie Li[b]

[a] State Key Laboratory of Fire Science, University of Science and Technology of China, Hefei, Anhui 230026, China
[b] Civil and Infrastructure Engineering Discipline, School of Engineering, RMIT University, Melbourne, VIC 3001, Australia

ARTICLE INFO

Article history:
Received 13 December 2017
Revised 7 April 2018
Accepted 10 April 2018
Available online 17 April 2018

Keywords:
Solar chimney
Optimization design
Natural ventilation
Fire safety
Smoke exhaustion
Renewable energy

ABSTRACT

Solar chimney has been primarily utilized for natural ventilation, but its application to smoke exhaustion was rarely explored. A 1:3 reduced-scale test platform with a dimension of 1.5 m × 1.5 m × 0.9 m (height) was used to optimize solar chimney under natural ventilation and smoke exhaustion, considering four influencing factors, including height of cavity inlet from the floor (0.2–0.8 m), cavity depth (2.5–17.5 cm), solar radiation (400–1200 W/m^2) and fire size (6.8–15.8 kW). Both natural ventilation and smoke exhaustion follow the same trend along the air inlet height and cavity depth, which confirms its viability on smoke exhaustion under fire condition without compromising the performance of natural ventilation. Experimental results suggested a chimney configuration of 0.5 m high air inlet and 12.5 cm cavity depth with optimized functions. External radiation shows obvious benefit on enhancing natural ventilation, while its influence on smoke exhaustion is limited. An empirical model was developed to predict the flow rate under normal and fire conditions. The outcomes of this study provide a technical guidance for the design of solar chimney under scenarios of both natural ventilation and smoke exhaustion.

1. Introduction

Energy usage and fire safety are the two inevitable aspects to maintain the functions of buildings. In Australia, the fire has caused approximately 100 fatalities and over 3000 injuries per year during 2004 and 2012, while the total cost of the fire was estimated at $12 billion or 1.3% of GDP [1]. At the same time, buildings represent nearly 40% of total energy usage and about half of the energy use are for heating, ventilation, and cooling [2,3]. The energy usage keeps increasing under the growing of building numbers and city expansions [4], while those conventional energy sources are difficult to fulfill such a heavy energy demand. Before the drying up of the conventional energy sources, many researchers and engineers then transfer their focuses to renewable energy.

A large number of studies have confirmed that smoke is the leading reason for fire casualties in buildings [5,6]. According to Australasian Fire Authorities Council [7], over 54% of fire deaths in Australia were due to smoke inhalation. Mechanical and natural smoke exhaustion systems are utilized in buildings to exhaust smoke under fire conditions [8]. The shortcomings of existing mechanical smoke exhaustion systems are requirements of the power supply and smoke detector, with an overall reliability of about 87.3% [9,10]. It means that approximately 12.7% of the systems cannot be activated during fire situations, which put occupants in big danger [11]. Existing natural smoke exhaustion system usually requires big opening, which may affect buildings' functions and aesthetics. Most importantly, the failure could be fatal when the openings are accidentally closed.

Solar chimney as a reliable renewable energy system has been largely utilized to conquer global energy crisis [12]. Usually, solar chimney cavity consists of a glazing wall and a thermal storage wall. Under solar radiation, the air in the cavity can be heated by the solar radiation penetrated through the glazing wall. Solar chimney can induce cooling or heating in building by natural ventilation based on solar radiation, without utilizing conventional energy sources. It shows advantages in terms of operational cost, energy requirement and carbon dioxide emission [13,14]. A building in Japan with solar chimney was found to reduce the fan shaft power requirement by about 50% in annual total due to the natural ventilation, even up to 90% in January and February [15].

Natural smoke exhaustion system is following the same principle with solar chimney, namely thermal buoyancy. The thermal buoyancy is caused by the density gradient of air due to different temperatures [16]. The characteristics of solar chimney

* Corresponding authors.
E-mail addresses: chengxd@ustc.edu.cn (X. Cheng), shilong@mail.ustc.edu.cn, long.shi@rmit.edu.au (L. Shi).

https://doi.org/10.1016/j.enbuild.2018.04.016
0378-7788/

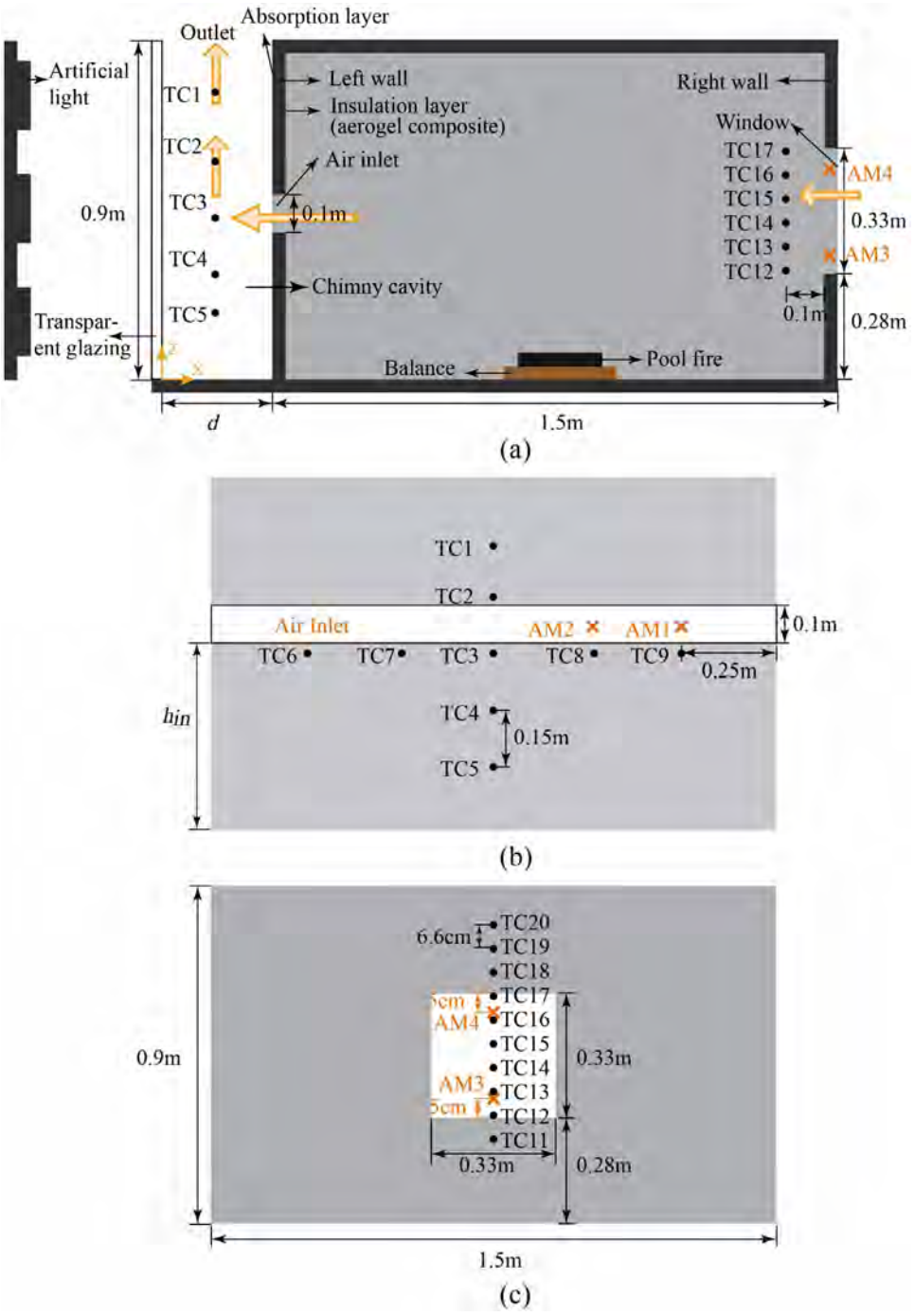

Fig. 1. A schematic view of the experimental platform in this study: (a) Experimental setup; (b) measurement spots in the middle plane of chimney cavity ($x = d/2$); and (c) measurement spots 0.1 m from the window ($x = d + 1.4$). TC (represented by filled circles) and AM (denoted by crosses) are thermocouple and anemometer, respectively.

provide an exceptional condition for smoke exhaustion. The air inlet and outlet of the solar chimney are always open without any cover, as seen in Fig. 1(a), while there is no need for the related alarm/activation system or mechanical component. Therefore, we can consider a 100% reliability of solar chimney in terms of smoke exhaustion. The smoke produced from the fire source can be exhausted to the outside environment through the solar chimney. Due to thermal buoyancy, the smoke exhaustion performance based on solar chimney may be better than those conventional natural smoke exhaustion systems. In this study, the performance of both natural ventilation and smoke exhaustion is defined by the volumetric flow rate through the solar chimney, which is a good indicator of air change per hour (ACH) and smoke exhaustion of buildings.

Based on our literature review on solar chimney [12,17], almost all the previous attempts have been focused on exploring its optimum design to enhance the natural ventilation under internal and external conditions. The designing factors include chimney configurations [18–22], installation conditions [23–25], material usages [14,26,27], and external environment [28–31]. Various types of mathematical models were also developed to predict the airflow rate in chimney cavity, including the predictions based on single factor [20,32], air temperature [33–35], air density [36], and external radiation [31,33,37]. All these studies showed that solar

chimney could largely enhance the natural ventilation in buildings with low construction cost and lifetime energy saving.

Besides its existing function of natural ventilation, using solar chimney for smoke exhaustion is still in an envisioning phase. Until now, only three studies have been found attempting to use the solar chimney for smoke exhaustion. In 2004, Ding et al. [38] initiated the idea and confirmed the possibility of using the solar chimney for smoke exhaustion in a building atrium. Later in 2006, Ding et al. [39] proved that both natural ventilation and smoke exhaustion could be realized by combining solar chimney with double-skin façade. In 2010, Chow and Chow [40] indicated that the higher surface temperature of a solar chimney wall might reduce the buoyancy of smoke. It is good to know from these studies that solar chimney can be used for both natural ventilation and smoke exhaustion. However, to the best of our knowledge, no study has been found in the literature regarding its optimum performance design in terms of natural ventilation and smoke exhaustion.

Therefore, a 1:3 reduced-scale experimental study was carried out to optimize the design of solar chimney for both natural ventilation and smoke exhaustion. The main objective of this study is to obtain the optimized performance of solar chimney under natural ventilation and smoke exhaustion conditions without compromising any one aspect. Several aspects were considered to explore their influences for the first time, including the height of cavity inlet from the floor, cavity depth, solar radiation and fire size. An empirical model was developed to predict the flow rate under both conditions, where it does not mean that both conditions happen at the same time. It means the solar chimney can be used for natural ventilation under normal conditions and once there is a fire it can be used for smoke exhaustion automatically. The outcome of this experimental study can provide a technical guide on solar chimney optimization design for both functions, which helps to create a safer and more sustainable home.

2. Experimental methodology

2.1. Experimental platform

A 1:3 reduced-scale experimental platform was built to carry out the experiment for natural ventilation under normal condition and smoke exhaustion under fire condition. The whole experimental setup contains three sub-systems: test room, artificial lights, and measurement system, as shown in Fig. 1. The solar chimney in this study is only for cooling purpose, while the details for the heating purpose can refer to Refs. [12,20].

The right section of Fig. 1(a) is the test room with a dimension of 1.5 m × 1.5 m × 0.9 m (height). The walls of the room were made of fire-proof board. There is an air inlet on the left wall, while the distance between its lower side and the floor can be adjusted considered as the vertical height of the air inlet, denoted by h_{in}. It should be mentioned during previous solar chimney studies, that the air inlet was usually located at the bottom of chimney cavity. After considering both the connected room and smoke exhaustion, we have tested different air inlet with various heights from the floor to address the optimization design of a solar chimney for natural ventilation and smoke exhaustion. The dimension of the air inlet keeps at 0.1 m (height) × 1.5 m (width). A window with a dimension of 0.33 m × 0.33 m is located at the center of the right wall. Its lower side is 0.28 m from the floor.

The left side of the test room is a solar chimney, constructed by the left wall of the test room and a transparent glazing on its left. The distance between the left wall and the glazing is usually expressed as the cavity depth (or cavity gap), represented by d. An aerogel composite board was attached to the right side of the left wall (fireproof board) for insulation purpose. From the observation during the fire experiments, the fireproof board is enough to stand the hot smoke under the analysed scenarios, as seen in Fig. 6(b), unless there is a direct entry of fire plume. After the chimney cavity is heated, the internal air rises under thermal buoyancy. The heated air is then exhausted to the outside environment through the outlet. After that, the air inside the test room is dragged into the cavity chimney for ventilation purpose.

The very left section of Fig. 1(a) is the artificial lights, including nine iodine-tungsten lamps with a 3 × 3 array. These lamps are used to simulate solar radiation, which can provide a uniform radiation heat on the glazing wall within a range of 0–2,000 W/m^2.

2.2. Measurement system

The measurement system mainly includes thermocouples (type k with 1 mm diameter) and an anemometer to measure the temperature and air velocity, respectively. As shown in Fig. 1(b), nine thermocouples (TC1–TC9) are put in the chimney cavity, represented by those filled circles. The horizontal distance between the two adjacent thermocouples is 0.25 m. The distance between TC9 (or TC6) and wall edge is also 0.25 m. The vertical distance between two adjacent thermocouples is 0.15 m, which also applies to the distance between TC1 (or TC5) and wall edge. These thermocouples are located in the middle plane between the glazing and left wall ($x = d/2$), and their positions are adjusted accordingly when d is changing.

To measure the temperature inside the room, a thermocouple tree was utilized, as shown in Fig. 1(c). These thermocouples, labeled as TC11-TC20, are located horizontally 0.1 m away from the window ($x = d + 1.4$). The top thermocouple is 0.808 m from the room floor. The vertical distance between the two adjacent thermocouples is 0.066 m.

A hot-wire anemometer (KANOMAX Model 1550/1560) with four channels (AM1-AM4) was used to measure the air velocities through the air inlet and window. The anemometer has a function of temperature compensation with an accuracy of ±7% full-scale reading under up to 80 °C, which is higher than the studied temperature in this study, as shown in Fig. 9. This kind of measurement accuracy is acceptable for the fire tests, especially for the studied scale of fire test under turbulent smoke. For those fire tests over the limit, it is suggested to use the correction method developed by Hultmark and Smits [41]. Due to the limited measurement spots, only half of the air inlet was measured, as shown in Fig. 1(b). AM1 is 0.25 m from the inlet end, while the distance between AM1 and AM2 is also 0.25 m. Both AM1 and AM2 are located along the vertical centreline of the inlet, which is also adjusted when h_{in} changes. The air (or smoke) velocity measurement at the air inlet is due to the quasi-symmetry of the problem. For the measurement spots AM3 and AM4, their positions are fixed with a distance of 0.05 m from the lower and upper sides of the window, respectively, as shown in Fig. 1(c).

2.3. Experimental procedure and scenarios

To provide a stable test environment, the experiments were taken in a big enough indoor laboratory. Two experimental conditions were tested in this study. The first is under normal condition, while only natural ventilation was considered during the experiment. The related tests are aiming to analyze the natural ventilation of solar chimney under the solar radiation. The second is under fire condition, where the performance of solar chimney for smoke exhaustion is tested. Diesel oil was used as the fire source, located at the center of the floor. Three square pans were used for the diesel oil, with side lengths of 0.12, 0.14, and 0.16 m, respectively. Below the pan, a balance with an accuracy of 0.01 g was used for the measurement of mass loss during the experiment. The measurement frequency of the balance is 1 Hz.

Table 1
A summary of test scenarios in this study.

Scenario No.	Height of air inlet (h_{in}, m)	Cavity depth (d, cm)	Solar radiation (q_s, W/m^2)	Fire size (q_f, kW)
1–7	0.2, 0.3, 0.4, 0.5, 0.6, 0.7, 0.8	5.0	800	6.8
8–13	0.5	2.5, 7.5, 10.0, 12.5, 15.0, 17.5	800	6.8
14–17	0.5	12.5	400, 600, 1,000, 1,200	6.8
18–20	0.5	15.0	800	6.8, 9.2, 15.8

Experiment contains several steps. First, the nine lamps were turned on and calibrated before the test to ensure they can provide a uniform radiation intensity on the glazing wall. The second step is mainly about the measurement of nature ventilation of the solar chimney under normal condition. After all the measured data are stable, the fuel pool located at the center of room floor was ignited, representing the start of smoke exhaustion under fire conditions. The transaction is following the practice that the solar chimney can automatically change from normal to fire conditions to exhaust smoke when a fire starts in the room. The test ends when the pool fire is extinguished.

To optimize the solar chimney design for both natural ventilation and smoke exhaustion, four parameters were tested through the experimental platform, including the height of air inlet (h_{in}, 0.2–0.8 m), cavity depth (d, 2.5–17.5 cm), solar radiation (q_s, 400–1,200 W/m^2), and fire size (q_f, 6.8–15.8 kW). The fire size was determined by the effective heat of combustion in the literature [42,43] and the measured average mass loss rate in this study. A summary of the test scenarios can be seen in Table 1. Each scenario was repeated once to address the repeatability of the experiments. This is due to the good repeatability of the experimental rig, with details shown below, and a large number of test scenarios.

As seen in Table 1, the influences of h_{in} on the performance were first undertaken through the experiment. From the results, it was obtained that the h_{in} of around 0.5 m shows good performance for both natural ventilation and smoke exhaustion. So h_{in} was fixed at 0.5 m during the following experiments for scenarios 8–20. This applies to the selection of cavity depth as well. The selection of solar radiation was based on the values close to practice [44], while for fire size it just simply started from the smallest one.

3. Results and discussion

3.1. Experimental outputs

Following the above experimental methodology, the main experimental outputs are the flow (air or smoke) velocity through the air inlet and the window, and the temperature inside the chimney cavity and near the window. Fig. 2 shows the experimental results regarding the repeatability of experiments, while the inlet height, cavity depth, solar radiation and fire size are 0.5 m, 10 cm, 800 W/m^2, and 6.8 kW, respectively. The output is average flow velocity of the two measurement spots (AM1 and AM2) through the air inlet, representing the flow rate through the air inlet due to the symmetry. It can be seen that the repeatability of the experiment is quite good under the test conditions of both natural ventilation and smoke exhaustion. After averaging the flow velocities every 6 seconds, to reduce those noises, the absolute uncertainties can be obtained by comparing those data from the two tests. It is known that the average absolute uncertainty is about 11.47%, which is better than those previous fire tests [45,46]. The uncertainty during the ignition period and near the extinguishment is quite high because of the relatively unstable conditions, which is the reason of selecting the time period (100–50 s before the ignition and 50–350 s after the ignition) for quasi-steady condition.

Each experimental run, as mentioned above, can be divided into two stages, namely natural ventilation and smoke exhaustion. The

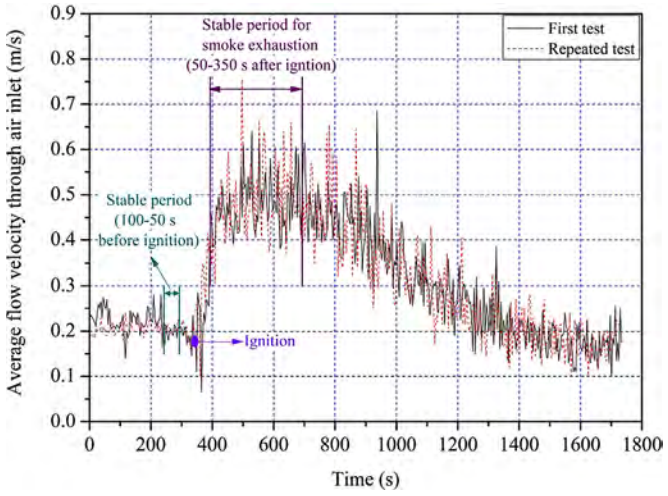

Fig. 2. Repeatability of experimental test. The inlet height, cavity depth, solar radiation and fire size are 0.5 m, 10 cm, 800 W/m^2, and 6.8 kW, respectively.

turning point is the ignition of the diesel pool, as shown in Fig. 2. During natural ventilation, the flow velocity shows a little fluctuation at the beginning and then becomes more stability during a later stage. It should be mentioned that the beginning of the data is not the start of the experiment as we begun to record the data when the data is relatively stable, same as below. After the ignition, a clear drop of the flow velocity can be observed from the reading. This is because the airflow circulation from the window to the chimney was temporarily blocked by the rising hot smoke. After that, the smoke velocity rises rapidly to a stable period (about 300 s). The smoke velocity then drops accordingly till the end.

Regarding the dropping of smoke velocity shown in Fig. 2, we hypothesized that the accumulation of the produced ash from the burning of diesel on the probe may affect the measurement. Based on this, a pure smoke exhaustion test was undertaken started from the fire ignition, and the results are presented in Fig. 3. It can be seen that the reading keeps stable for about 300 s and then drop accordingly along the time. At about 1100 s, we brushed the probe of the anemometer, and a clear rising can be observed after that. To confirm this phenomenon, we took another brushing at around 1300 s and the rapid rising was still presented after that. Therefore, it is indicated that the accumulation of the ash on the probe can affect the measurement of the flow velocity. From Fig. 3, it can be also seen that the smoke velocity can keep at those values even after 1300 s.

Considering all the experimental runs in this study, the period of 100–50 s before ignition can be considered as a relatively stable stage for natural ventilation under normal condition, as shown in Fig. 2. Similarly, 50–350 s after the ignition can be considered as a relatively stable period for the smoke exhaustion under fire condition. We didn't consider the period till the end because the accumulation of ash on the probe can affect the measurement, as shown in Fig. 3, while a 300 s period is appropriate based on all the experimental runs. Therefore, the data within these two periods were selected for further analysis in the following con-

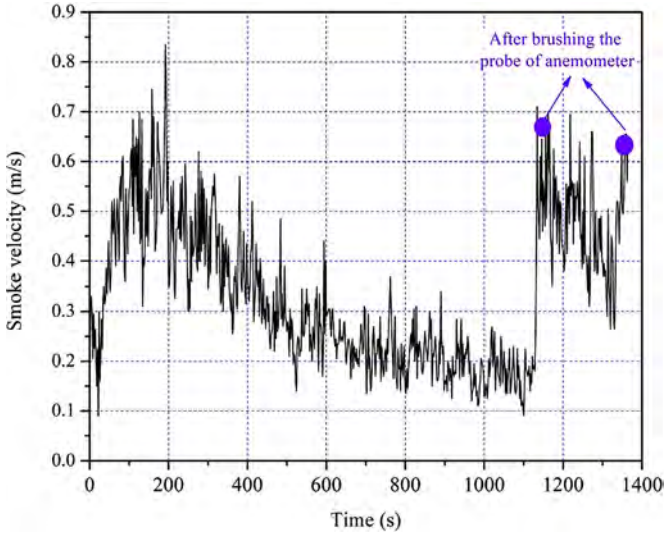

Fig. 3. Measurement of smoke flow velocity after brushing the probe of the anemometer.

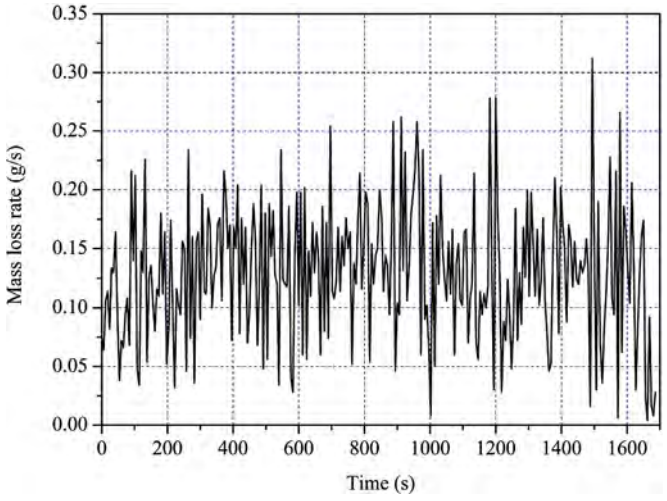

Fig. 4. Mass loss rate history of 12 cm square diesel pool fire with 0.5 m air inlet height and 5 cm cavity depth under 800 W/m^2 radiation.

tents, representing natural ventilation and smoke exhaustion. The average flow velocity in the following contents means the average measurements during these two periods, unless specified.

It is worth mentioning that the fire source is quite stable during the whole experiments. Fig. 4 shows the mass loss rate history of 12 cm square diesel pool fire with 0.5 m air inlet height and 5 cm cavity depth under 800 W/m^2 radiation. It can be seen that the diesel fire is quite stable after the ignition, which keeps at around 0.13 g/s during the whole experimental period. As the smoke production is much dependent on the mass loss rate, it indicates that the diesel pool is a good source to produce constant smoke along the time. This is because the size of pool fire is much dependent on the surface area, which can keep at a stable value until out of fuel [47,48].

The mass loss rate history of diesel pool fire under other experimental scenarios was also recorded. Fig. 5 shows the average mass loss rate of diesel fire under the effects of air inlet height and cavity depth. It can be observed that the average mass loss rate can keep around a fixed value even under various inlet heights and cavity depths. Although there is a little fluctuation under several cavity depths, it can be seen that the diesel pool fire can provide an equivalent smoke production even under different scenarios. This is much because the window from the left side, as seen in Fig. 1(a), can supply enough oxygen to sustain the pool fire, and the pool fire in this study can be considered as fuel-based combustion. There is a little jump in average mass loss rate when the cavity depth is about 5 cm. As the air supply is quite enough to support the burning process, this might be because of the relatively unstable characteristics of the liquid pool fire when it approaching the extinguishment that about 200 s earlier than the other scenarios.

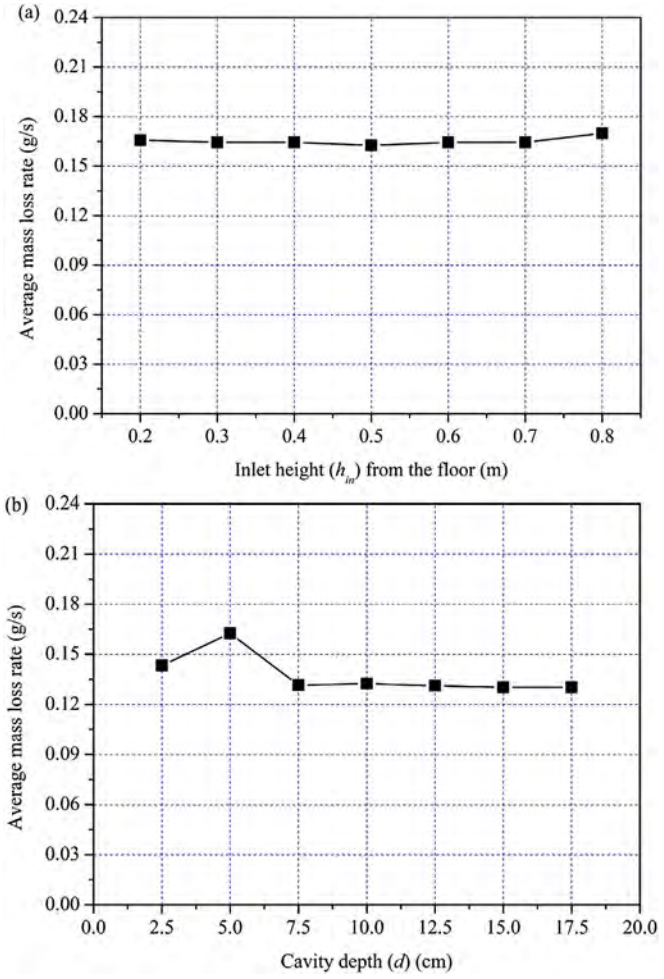

Fig. 5. Average mass loss rate of diesel fire under effects of: (a) inlet height; and (b) cavity depth.

Temperatures inside the cavity and near the window were also measured by thermocouples for 0.5 m high air inlet and 17.5 cm thick cavity under 800 W/m^2, as seen in Fig. 6. It should be mentioned that $t = 0$ is not the start of the experiment that we started recording after the data show relatively stable outputs. So the start of the data is just the beginning of the recording, not the ambient temperature, which is the reason why they show different outputs at the very beginning.

Fig. 6(a) shows the temperature profile inside the cavity. It can be observed for those thermocouples below the air inlet, namely TC4 and TC5, their temperatures are higher than the others at natural ventilation stage. This is because the air can absorb the radiation from left-side artificial lights but with limited convective heat loss when its movement is restricted below the air inlet in the chimney cavity. It does not mean that the air keeps still all the time, which can be proved by the temperature during smoke exhaustion stage. Both TC4 and TC5 show a higher temperature than those under natural ventilation stage, indicating the entry (reserve

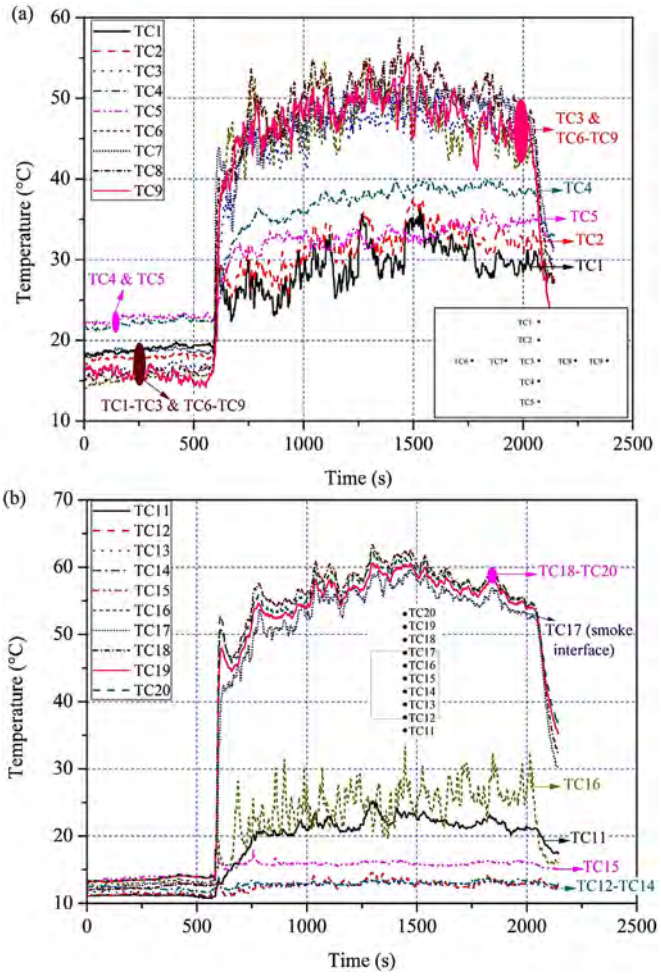

Fig. 6. Temperature histories for locations: (a) inside the chimney cavity; and (b) near the window.

flow) of hot smoke in the area. However, the reserve flow of the smoke could not affect the performance much as there is limited air movement without obvious circulation in the places.

For the thermocouples above the air inlet, namely TC1 and TC2, their temperatures are lower than TC4 and TC5 because of the high convective heat loss under the high flow rate at the natural ventilation stage. However, during the smoke exhaustion stage, their temperatures seem to be still relatively lower. This is because of the reserve flow of fresh air from the cavity top when the cavity depth is relatively big under the circumstance (17.5 cm here). After narrowing the chimney cavity, it is observed that the temperature measured by TC1 and TC2 increase gradually, indicating the less reverse flow of fresh air. The details will be given in the following sections.

The temperature outputs from TC3 and TC6-TC9 are quite straightforward, as shown in Fig. 6(a). During the natural ventilation stage, they show a relatively lower temperature because of the convective heat loss occurred during the movement. After the ignition, the temperatures are quite high because they are facing the hot smoke from the air inlet. Their temperatures are also a slightly lower than those of smoke layer inside the room, as shown in Fig. 6(b). It is because of the heat losses due to the radiation and convection during the movement.

Fig. 6(b) shows the temperature outputs inside the room and 0.1 m from the window under various heights. Under natural ventilation, the outputs show slightly different temperature because of the movement of air flow and different measurement locations. After the ignition, the temperatures from those thermocouples near the ceiling increase rapidly. The produced smoke from the fire source rise up under thermal buoyancy and was gathered near the ceiling. The smoke layer drops accordingly when more smoke is produced. From the temperature outputs, a clear smoke layer can be known at 0.61 m (the height of TC17) from the floor, which can be judged from the temperature differences between TC16 and TC17.

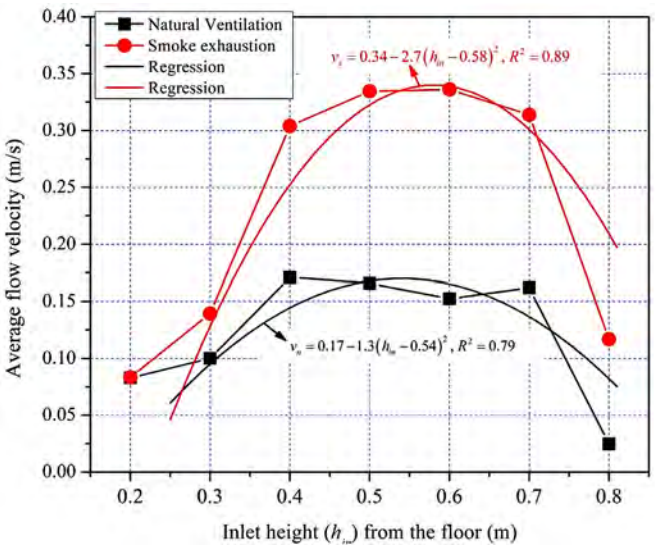

Fig. 7. Influences of inlet height on natural ventilation and smoke exhaustion for a 5 cm cavity depth under a radiation of 800 W/m^2. The fire size is 6.8 kW.

For those thermocouples at window height, the temperature outputs are much dependent on the interaction of the smoke and fresh air supplied from outside environment. For this case, it can be known that the window is much focusing on fresh air supply, but not the smoke exhaustion. This is because the temperature measurements from TC12 (same height of window sill) to TC15 (0.132 m below the window head) are much lower than the smoke temperature. Although there will be a possibility of both flowing in or out, the air through the lower part of the lower part of the window should be flowing out, otherwise, the mass of the whole system could against the mass conservation law that all the openings are for exhaustion. Temperatures from TC11 (below the window sill) and TC16 (0.066 m below the window head) are a little higher because of the outgoing flow of the hot smoke at the upper part of the room. The function of the room in this study is similar to those under single-sided natural ventilation [49,50]. More detailed analysis about the window will be given in the following sections.

3.2. Chimney configuration

Although many previous studies have addressed the influences of air inlet size on solar chimney performance [12], very few studies have been found on air inlet height (from the floor), not to mention smoke exhaustion under fire condition. Chimney depth as an important factor has been frequently investigated [28,51], while no study has been found in the literature regarding its smoke exhaustion performance. This section will mainly serve the purpose of addressing the influences of these two factors on the performance of both natural ventilation and smoke exhaustion.

Fig. 7 shows the influences of inlet height on the average flow (airflow or smoke) velocity through air inlet under normal and fire conditions for a 5 cm cavity depth under a radiation of 800 W/m^2. The pool fire is 12 cm square, representing a 6.8 kW fire. The peri-

ods to obtain the average data can be seen in Fig. 2, and the average data are the average measurements from two probes, which are appropriate to represent the flow rate through the air inlet. It can be observed from natural ventilation that the average flow velocity increases gradually to the maximum when inlet height rises from 0.2 m to 0.4 m. After that, the velocities fluctuate a little bit but all are above 0.15 m/s until an air inlet height of 0.7 m. When the inlet moves to a height of 0.8 m, the average velocity reduces rapidly.

Under normal condition, the trend of air velocity under various air inlet heights is determined by two factors: (a) the resistance (pressure loss) of flow from window to the air inlet; and (b) thermal buoyancy effect inside the chimney cavity. When the air inlet rises from 0.2 m to above, the part of cavity below the air inlet becomes less important because limited flow movement happens there, considering as the reduced heated area (A_{hot}). The limited flow movement even the reserve flow can be obtained by temperature profile shown in Fig. 6(a). Our previous study [52] indicated that the inlet air flow is proportional to the $A_{hot}^{1/3}$. So the thermal buoyancy effect reduces when the air inlet is moving up. At the same time, the pressure loss reduces as well when the window and air inlet have a similar height that it is easier for air flow entering the cavity through the air inlet [33].

When the air inlet keeps moving up, there should be a balance between these two factors when the reduced thermal effect and pressure losses are equal. The results from Fig. 7 prove this, which shows that the average flow velocity increases from 0.083 to 0.1 m/s when the air inlet rises from 0.2 to 0.3 m, and to the maximum when it rises to 0.4 m. After that, the velocity drops a little bit but always higher than 0.15 m/s. It is known from this phenomenon that the window may play a more important role in determining the overall performance. This is because when the air inlet rises from 0.4 to even 0.7 m (with only 0.2 m effective heated wall left), the velocity does not drop much. The increased inlet height of 0.3 m (from 0.4 to 0.7 m) is very close to the window size, namely 0.33 m. When the air inlet rises to 0.8 m (the top), both the dropped thermal buoyancy effect and increased pressure losses result in a sharp decrease of the velocity, namely from 0.162 to 0.025 m/s.

The trend for smoke exhaustion is also similar, as shown in Fig. 7. The inlet heights with similar flow velocities to the maximum are also located within 0.4–0.7 m, but the maximum happens at 0.5 (or 0.6 m as they are very close). It is a little higher than that of natural ventilation. This is because the hot smoke can rise up under thermal buoyancy, while a little higher air inlet can benefit the entry. Therefore, different from natural ventilation, when the air inlet drops from 0.7 to 0.8 m, the flow velocity does not reduce to nearly zero like the natural ventilation.

The effects of cavity depth on solar chimney performance were also investigated within a range of 2.5–17.5 cm. Cavity depth shows a similar influence on both smoke exhaustion and natural ventilation, as shown in Fig. 8. The airflow rate inside the cavity not always increases with a bigger cavity. The velocity of both air and smoke increases when the cavity depth rises from 2.5 to 12.5 cm, and it decreases after that. For both natural ventilation and smoke exhaustion, the maximum happens when the cavity depth is 12.5 cm. Lee and Strand [28] also obtained a similar result based on numerical modeling that when the cavity depth increases from 0.15 to 0.75 m, the air flow rate decreases by 1.9–4.7% in three United States cities.

The existence of the critical cavity depth of 12.5 cm in this study is because of the reverse flow [12]. As the heating processes of the air inside the cavity are much dependent on convective heat transfer, the air adjacent to the heated wall is prone to be heated. The heat transfer from the heated wall to the movable air in the middle of the cavity is relatively limited for a big cavity. Temperature difference and frictions between the two air layers are the two main reasons for reverse flow. The bigger the cavity is, the more obvious the reserve flow will be. This can be proved by the temperature outputs of TC1 (the thermocouple at the cavity top), as shown in Fig. 9(b). The smoke temperature keeps decreasing with a bigger cavity depth. The reduced temperature is because of the mixture of ambient air (reserve flow from the outside) and the hot smoke. A lower temperature indicates a more serious mixture of the ambient air.

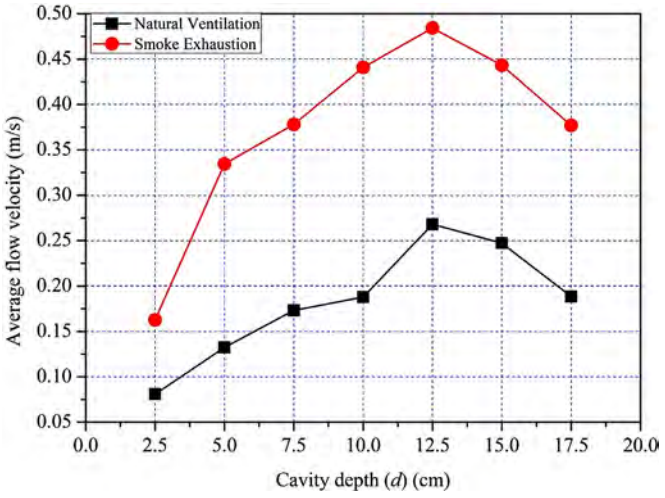

Fig. 8. Influences of cavity depth on natural ventilation and smoke exhaustion for a 0.5 m high air inlet with radiation and fire size are 800 W/m^2 and 6.8 kW, respectively.

Fig. 9(a) shows the temperature output of TC1 under the effects of air inlet height with a cavity depth of 5 cm. It can be seen that the temperature rises gradually when the inlet height increases from 0.2 to 0.4 m. This is because of the heat losses between smoke and the cavity walls during its rising process. When the air inlet is higher than 0.4 m, the temperature keeps almost the same, showing an unobvious trend. This is because TC1 is almost directly facing the hot smoke from the air inlet under such heights. It is also indicated that the reserve flow is very limited as there is no obvious temperature drop comparing to the smoke layer in the room, as shown in Fig. 6.

For the natural ventilation, the related outputs in Fig. 9 were not addressed due to two reasons. The first is that the related experimental studies on the reserve flow of natural ventilation are quite well analysed previously [12], which also shows similar trends with the smoke exhaustion in the above analysis. The second is that the outputs among the different scenarios are quite low and similar, while different ambient temperatures for these tests may affect the outputs to some extent as well.

Based on above analysis, it is known that solar chimney can be used for natural ventilation and smoke exhaustion under normal and fire conditions, respectively. Regarding the chimney configuration, the performance of both natural ventilation and smoke exhaustion follows the same trend, which greatly enables the solar chimney on smoke exhaustion under fire condition without compromising the performance of natural ventilation. To optimize the performance of both functions, a chimney configuration of 0.5 m high air inlet and 12.5 cm cavity depth are suggested for the tested room configuration in this study.

3.3. Environmental factors

In this section, environmental factors including external radiation and internal fire size on the performance of natural ventilation

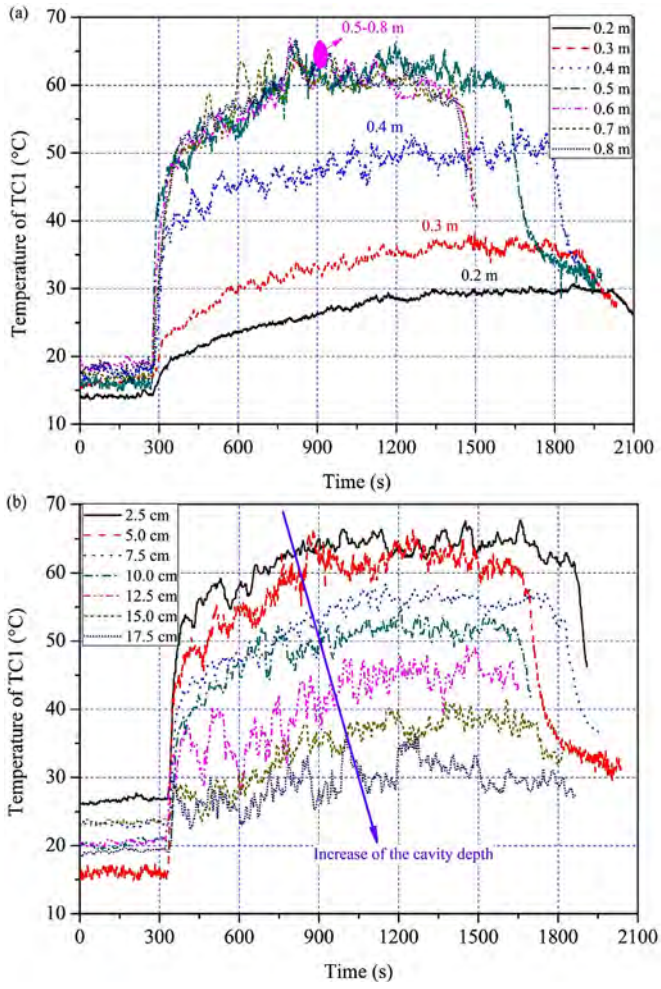

Fig. 9. Temperature near the cavity top (TC1) under the effects of: (a) air inlet height with a cavity depth of 5 cm; and (b) cavity depth with an air inlet height of 0.5 m.

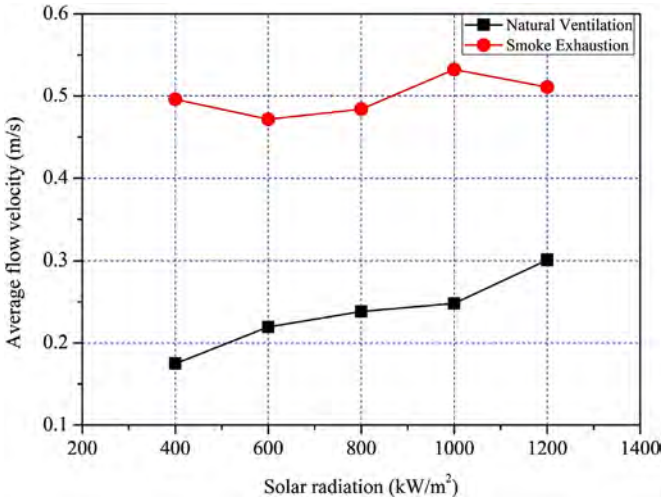

Fig. 10. Influences of solar radiation on natural ventilation and smoke exhaustion.

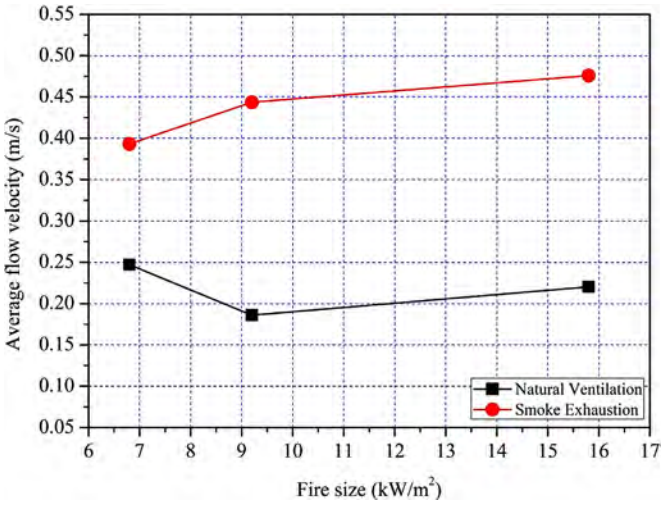

Fig. 11. Influences of fire size on natural ventilation and smoke exhaustion.

and smoke exhaustion will be addressed through the experimental outputs. In terms of the external radiation, the trend is quite clear for natural ventilation that the performance of solar chimney is enhanced with a higher external radiation, as shown in Fig. 10. This is because it provides the energy to heat up the air inside the chimney cavity, which is the source for thermal buoyancy. Chen et al. [23] and Bansal et al. [53] also indicated the same result that the airflow rate was found rising with the increase of heat flux.

Before the experiments, the smoke exhaustion under fire conditions was expected to follow the same trend. However, according to Fig. 10, the external radiation seems to show unobvious influences on smoke exhaustion. Average smoke velocity through the air inlet drops from 0.496 to 0.472 m/s when the radiation heat flux increases from 400 to 600 W/m^2. Another drop can be also seen when radiation rises from 1000 to 1200 W/m^2. They seem to fluctuate within a range of 0.5 ± 0.033 m/s, which indicated that the external radiation shows limited influence on the smoke exhaustion. This is probably because of the high temperature of smoke. As seen in Fig. 6(a), the temperature of hot smoke through the air inlet (TC3 & TC6–TC9) are as higher as 55 °C, which is much higher than the heated air of about 22 °C in the cavity (TC4 & TC5). So the thermal buoyancy of the hot smoke itself is much stronger than the heated air by external radiation in the cavity.

Similarly, the influence of fire size on the natural ventilation can be ignored because the data measurement was taken before the ignition of diesel pool fire, as seen in Fig. 11. The average flow velocities are located with a range of 0.218 ± 0.03 m/s, which is considered as an acceptable level of error from repeated tests.

As can be seen from Fig. 11 that there is no obvious difference for the average flow velocities under three fire sizes, there shows an increasing trend when the fire size increases. It may indicate that the airflow rate through the solar chimney increases with a bigger fire size, under the compromise of the smoke exhaustion through the window. This is because when the pool sizes increase from 12 to 14 cm, more smoke was released from the fire source. The temperature of the smoke layer would be higher. This can be proved by previous experiments [54,55].

The temperature profiles near the window were also measured by the thermocouples (TC12-TC17), which is an important indicator of window's function during natural ventilation and smoke exhaustion. Fig. 12(a) shows the temperature profiles near the window under a cavity depth of 5 cm. It can be observed that the temperatures measured by TC16 (0.066 m below the window head) and TC17 (window head) are approaching the smoke temperature, indicating smoke exhaustion through the window. As the temperature of TC15 (0.132 m below the window head) is near the ambient temperature, it means that smoke exhaustion happens within a small gap of less than 0.132 m near the window head. It can be known that the window is mainly for ambient air supply under fire

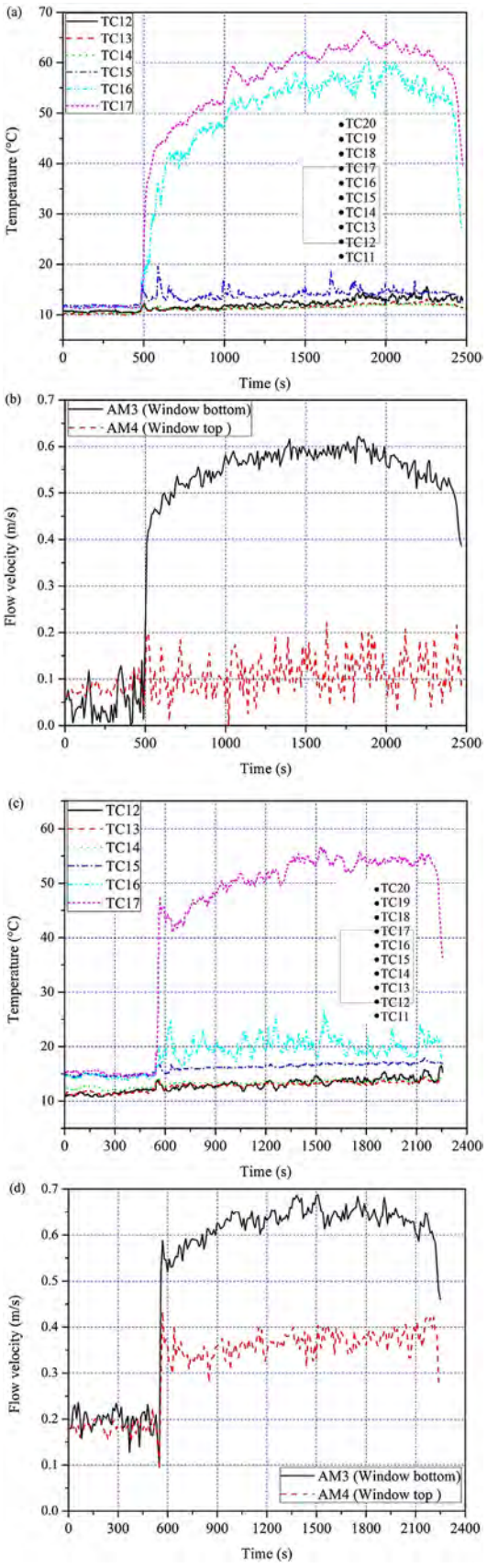

Fig. 12. Temperature and flow velocity profiles near the window for: (a)–(b) 0.5 m high air inlet and 5 cm cavity depth; and (c)–(d) 0.5 m high air inlet and 12.5 cm cavity depth.

conditions. Following the mass conservation law under the quasi-steady conditions, the mass flux of the air supply through the bottom window should be equal to the summation of the mass flux through the chimney cavity and the upper window.

After increasing the cavity depth, as shown in Fig. 12(c), it was noticed that only the temperature measured by TC17 was approaching smoke temperature, indicating the smoke layer at a height between 0.544 m (TC16) and 0.61 m (TC17). So smoke exhaustion only happen through a very small portion of the upper window, namely less than 0.066 m. This is much because of the enhanced performance of solar chimney for smoke exhaustion, which is evidenced by Fig. 8.

Based on the above temperature outputs, it is noticed that the window is mainly for supplying ambient air from outside, but not exhausting the smoke. The velocity outputs can also confirm this, as seen in Fig. 12(b) and (d). It can be observed from these two figures that the velocity of flow-in ambient air near the window bottom is much higher than that of the smoke exhaustion through the upper window. Based on mass conservation theory, the different mass of the flow-out and flow-in mass is equal to the mass of those exhausted smoke through the solar chimney. It should be noticed that even the velocity difference in Fig. 12(b) is higher than that in Fig. 12(d), the performance under 12.5 cm is better because of the changed portions of the window for air supply and smoke exhaustion.

Based on above analysis, it can be seen that the external radiation shows obvious benefit on enhancing the natural ventilation under normal condition, while its influence on the smoke exhaustion under fire condition is limited. The performance of smoke exhaustion shows an enhanced trend under a bigger fire. In addition, it can be noticed that the window under the fire conditions is mainly for ambient air supply, but not for smoke exhaustion.

4. Development of empirical model

In this section, an empirical model will be developed to predict the performance of solar chimney, including both natural ventilation and smoke exhaustion. As both natural ventilation and smoke exhaustion were considered in the experiment, the objective is to develop the model which can predict the flow rate under the two conditions. The reason for developing an empirical model is to benefit the practical usage by largely reducing the time cost, while it can simply show the quantitative relationship between the performance and influencing factors.

As a 1:3 reduced-scaled experimental test rig was used for this study, Froude modelling was then applied to expand the application from reduced-scale to full-scale. Froude modelling is much based on Froude number (Fr), which is calculated by $Fr = V^2/gH$. The principle of Froude modelling is to address the relationship among different scaled tests by holding the Froude number constant [54,56–59]. For the parameters such as length, velocity and fire size (or the related), the relationships can be given by,

$$L_r = \frac{H_m}{H_r} L_f \tag{1a}$$

$$v_r = \left(\frac{H_r}{H_f}\right)^{1/2} v_f \tag{1b}$$

$$Q_r = \left(\frac{H_r}{H_f}\right)^{5/2} Q_f \tag{1c}$$

where L represents the length, m; H is the height of the room or chimney cavity, m; v is the velocity, m/s; Q is the fire size or the heat-related variables, W; and subscripts r and f represent reduced-scale and full-scale, respectively.

A theoretical model was developed by Andersen [33] to predict the airflow of a room (or cavity) with multiple openings. This model has been frequently used to predict the performance of solar chimney as it is based on the same configuration and mechanism. The model is applicable to the case for a room with vertical, horizontal, or combined openings. The model can be expressed by:

$$V = 0.038(Q_{\text{total}}H_n)^{1/3}(C_dA_{\text{out}})^{2/3} \quad (2)$$

where V is the air flow rate at the outlet, m^3/s; Q_{total} is the total heat absorbed by the air in the cavity, W; H_n is the vertical distance between the outlet and neutral plane, m; C_d is the discharge coefficient; and A_{out} is the outlet area, m^2.

Under normal condition, the heat provided for the natural ventilation is mainly based on the solar radiation. It can be seen from Fig. 6(a) that the movement of the bottom part of the air inside the cavity below the air inlet is limited. It means that not all the part of heat absorption is used to promote natural ventilation. The energy used for natural ventilation can be expressed by:

$$Q_{\text{rad}} = \tau wH\dot{Q}''_{\text{rad}} \quad (3)$$

where Q_{rad} is the radiation heat, W; w is the width of the chimney cavity, m; $\dot{Q}''_{\text{rad}}$ is the radiation intensity, W/m^2; and H is the total height of chimney cavity, m; τ is the transmissivity of the glazing wall, which is 0.78 in this study [60].

When the solar chimney transfers to fire mode, besides the solar radiation, the heat absorbed by the air also comes from the fire source. The fire source is also providing the energy to heat the air (smoke) inside the cavity, showing equivalent effect with the solar radiation. In addition, as seen in Fig. 12, a part of the smoke exhaust to the outside through the window, which is the part of energy not involved the solar chimney function. Under the stable condition, we assumed that the part of smoke exhaust through the solar chimney is fixed. So the heat absorbed from the fire source for the air (smoke) inside the cavity can be estimated by:

$$Q_{\text{fire}} = \xi wH\dot{Q}''_{\text{fire}} \quad (4)$$

where Q_{fire} is the exhausted heat from fire source, W; $\dot{Q}''_{\text{fire}}$ is the fire size (also called heat release rate), W/m^2; and ξ is the coefficient considering the portion of smoke through the window and also scaling the fire size to the same area with the solar absorption.

Based on Eqs. (3) and (4), the total heat absorbed by the air (smoke) in the cavity can be estimated by:

$$Q_{\text{total}} = wH\left(\tau\dot{Q}''_{\text{rad}} + \xi\dot{Q}''_{\text{fire}}\right) \quad (5)$$

The vertical distance between the outlet and neutral plane, H_n, is considered proportional to the total cavity height:

$$H_n = C_1 \cdot H \quad (6)$$

where C_1 is the coefficient, which is considered fixed [33].

The outlet area is calculated by:

$$A_{\text{out}} = wd \quad (7)$$

where w is the cavity depth, m.

Therefore, based on above equations, the air flow rate at the outlet can be calculated as follows:

$$V = C_2\left[d^2H^2w^3\left(\tau\dot{Q}''_{\text{rad}} + \xi\dot{Q}''_{\text{fire}}\right)\right]^{1/3} \quad (8)$$

where C_2 is the empirical coefficient which can be obtained based on experimental data.

Eq. (8) is the empirical model without considering the effects from the window. Based on Fig. 7, it was known that a parabolic curve is shown between the air (smoke) velocity and the inlet height. So a relationship is assumed:

$$v_w = \left[C_3 - C_4(h_{\text{in}} - C_5)^2\right]v \quad (9)$$

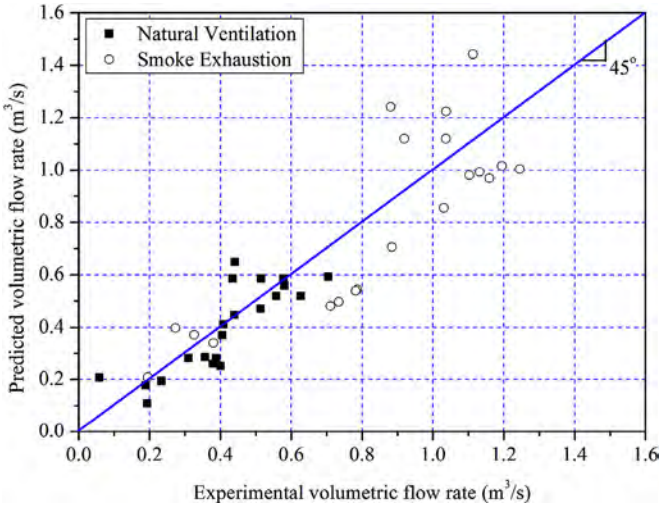

Fig. 13. Validation of the empirical model of this study. The experimental data were converted to full-scale before the comparison.

where v_w and v are the air velocity through the inlet considered and without considering the window, respectively, m^3/s; and C_3, C_4, and C_5 are the coefficients.

The coefficients in Eq. (9) can be obtained based on regression of experimental data shown in Fig. 7. The relationships for natural ventilation and smoke exhaustion can be obtained, respectively:

$$v_n = 0.17 - 1.3(h_{\text{in}} - 0.54)^2, \qquad R^2 = 0.79 \quad (10a)$$

$$v_s = 0.34 - 2.7(h_{\text{in}} - 0.58)^2, \qquad R^2 = 0.89 \quad (10b)$$

where v_n and v_s are the flow velocities through the air inlet under natural ventilation and smoke exhaustion conditions, respectively, m/s.

We can know from above equations that the coefficient of determination (R^2) for the regression is higher than 0.79, which is not so high but acceptable for this study. To consider both natural ventilation and smoke exhaustion, an average value of 0.56 is then selected for the coefficient shown in the bracket. Considering the scaling law shown in Eqs. (1a)–(1c), the relationship between the velocity and air inlet height can be given for full-scale model,

$$v = C_5 - C_6(h_{\text{in}} - 1.68)^2 \quad (11)$$

where C is the coefficient, which can be obtained from experimental data.

After considering the window, the air (smoke) volume rate of the solar chimney can be expressed by:

$$V_w = C_7\left[C_8 - (h_{\text{in}} - 1.68)^2\right]w(dH)^{2/3}\left(\tau\dot{Q}''_{\text{rad}} + \xi\dot{Q}''_{\text{fire}}\right)^{1/3} \quad (12)$$

Based on the regression of the experimental data in this study, the coefficients in Eq. (12) can be obtained. Eq. (12) can be rewritten as:

$$V_w = 0.0029\left[1.88 - (h_{\text{in}} - 1.68)^2\right]w(dH)^{2/3}\left(\tau\dot{Q}''_{\text{rad}} + 0.55\dot{Q}''_{\text{fire}}\right)^{1/3} \quad (13)$$

It should mention that a ξ of 0.55 is quite consistent with the above result that the window is mainly for fresh air supply, but not smoke exhaustion. The validation of the empirical model is shown in Fig. 13. It can be seen that those predictions fit reasonably well with the experimental data in this study. The average error for the comparison between the predictions and experiments is about 24.7%. Compared with smoke exhaustion, the prediction accuracy of the natural ventilation seems better. This may be due

to the complicated fire condition of fluctuated fire developed, as shown in Fig. 4.

Since the experiment in this study only considered the fixed areas of air inlet and window, the empirical model shown in Eq. (13) has some limitations. For example, reserve flow may happen near the outlet due to the uneven heating process when the cavity gap keeps increasing. Ong and Chow [61] stated that no reverse air flow circulation was observed even at a large gap of 0.3 m, while Chen et al. [23] confirmed the reverse flow occurring from chimney outlet for a 0.4 m cavity gap through flow visualization experiment. As seen from Fig. 13, the experimental volumetric flow rate obtained by Mathur et al. [62] for an up to 0.3 m cavity gap can be well predicted by the developed model. Therefore, it is suggested that the developed empirical model can be used for a solar chimney with an up to 0.3 m cavity gap.

To apply this model to various air inlet and window, more experiments need to be carried out. We also tried to include as many as possible other experimental data from the references for the validation. However, very few experimental data are available for solar chimney attached to a room with a window. To the best of our knowledge, this is the first study which experimentally addresses the effects of some design parameters on the solar chimney performance considering both natural ventilation and smoke exhaustion. Therefore, no other experimental data can be found in the literature to validate the empirical model under fire conditions.

5. Conclusions

Although solar chimney, as a reliable renewable energy system, has been widely utilized for natural ventilation, their applications on smoke exhaustion under fire condition were rarely explored. In this study, a 1:3 reduced-scale test platform with a dimension of 1.5 m × 1.5 m × 0.9 m (height) was used to optimize the design of solar chimney on both natural ventilation and smoke exhaustion. Several aspects were considered to explore their influences on both functions for the first time, including the height of cavity inlet from the floor (0.2–0.8 m), cavity depth (2.5–17.5 cm), solar radiation (400–1,200 W/m^2) and fire size (6.8–15.8 kW).

Regarding the chimney configuration, the performance of both natural ventilation and smoke exhaustion follows the same trend, which enables solar chimney on smoke exhaustion under fire conditions without compromising the performance of natural ventilation. To optimize the performance under these two conditions, a chimney configuration of 0.5 m high air inlet and 12.5 cm cavity depth was adopted for the tested room configuration in this study. External radiation shows obvious benefit on enhancing the natural ventilation under normal condition, while its influence on the smoke exhaustion under fire condition is limited. In addition, the experimental results indicate that the window under the fire conditions was mainly for ambient air supply, not for smoke exhaustion.

An empirical model was developed to predict the flow rate through air inlet under both normal and fire conditions. The predictions are fitting well with experiments. This empirical is targeting both smoke exhaustion (defining the related fire size through $\dot{Q}''_{\text{fire}}$) and natural ventilation (defining $\dot{Q}''_{\text{fire}} = 0$). The model can be expressed as:

$$V_w = 0.0029\left[1.88 - (h_{\text{in}} - 1.68)^2\right] w(dH)^{2/3}\left(\tau \dot{Q}''_{\text{rad}} + 0.55\dot{Q}''_{\text{fire}}\right)^{1/3}$$

The results predicted by the empirical model compare well with experimental results. Due to the reserve flow happens near the outlet, it is suggested that the empirical model can be used for a solar chimney with an up to 0.3 m cavity gap. The research outcome can provide a technical guide to the design of solar chimney in single story buildings, and also mid- and high-rise building. For multiple-storey building, the relevant outcomes such as cavity depth and air inlet height are still applicable. Our future works will be the performance under variable air inlet and window.

Acknowledgment

This work was supported by National Key Research and Development Program of China (no. 2016YFC0800603) and Fundamental Research Funds for the Central Universities under grant (no. WK2320000035). We sincerely appreciate these supports.

References

[1] B. Ashe, J. McAneney, The real cost of fire in Australia, World Fire Stat. Bull. 28 (2012) 1–3.
[2] H.R. Li, Y.B. Yu, F.X. Niu, M. Shafik, B. Chen, Performance of a coupled cooling system with Earth-to-air heat exchanger and solar chimney, Renewable Energy 62 (2014) 468–477.
[3] Y.X. Chen, L.X. Gu, J.S. Zhang, EnergyPlus and CHAMPS-multizone co-simulation for energy and indoor air quality analysis, Build. Simul. 8 (2015) 371–380.
[4] Y.X. Chen, T.Z. Hong, M.A. Piette, Automatic generation and simulation of urban building energy models based on city datasets for city-scale building retrofit analysis, Appl. Energy 205 (2017) 323–335.
[5] Y. Alarie, Toxicity of fire smoke, Crit. Rev. Toxicol. 32 (2002) 259–289.
[6] W.M. Pitts, The global equivalence ratio concept and the formation mechanisms of carbon monoxide in enclosure fires, Prog. Energy Combust. Sci. 21 (1995) 197–237.
[7] Australasian Fire Authorities Council. Accidental fire fatalities in residential structures: who's at risk? 2005.
[8] T.X. Qin, Y.C. Guo, C.K. Chan, W.Y. Lin, Numerical simulation of the spread of smoke in an atrium under fire scenario, Build. Environ. 44 (2009) 56–65.
[9] G.Q. Chu, T. Chen, Z.H. Sun, J.H. Sun, Probabilistic risk assessment for evacuees in building fires, Build. Environ. 42 (2007) 1283–1290.
[10] R. Jonsson, J. Lundin, in: The Swedish Case Study: Different Fire Safety Design Methods Applied on a High Risk Building, Lund University, Sweden, 1998, pp. 29–35.
[11] L. Shi, R.F. Zhang, Q.Y. Xie, L.H. Fu, Improving analytic hierarchy process applied to fire risk analysis of public building, Chin. Sci. Bull. 54 (2009) 1442–1450.
[12] L. Shi, G.M. Zhang, W. Yang, D.M. Huang, X.D. Cheng, S. Setunge, Determining the influencing factors on the performance of solar chimney in buildings, Renewable Sustainable Energy Rev. 88 (2018) 223–238.
[13] X.Q. Zhai, Z.P. Song, R.Z. Wang, A review for the applications of solar chimneys in buildings, Renewable Sustainable Energy Rev. 15 (2011) 3757–3767.
[14] D.S. Lee, T.C. Hung, J.R. Lin, J. Zhao, Experimental investigations on solar chimney for optimal heat collection to be utilized in organic Rankine cycle, Appl. Energy 154 (2015) 651–662.
[15] T. Miyazaki, A. Akisawa, T. Kashiwagi, The effects of solar chimneys on thermal load mitigation of office buildings under the Japanese climate, Renewable Energy 31 (2006) 987–1010.
[16] R. Khanal, C.W. Lei, Numerical investigation of the ventilation performance of a solar chimney, ANZIAM J. 52 (2011) 899–913.
[17] L. Shi, M.Y.L. Chew, A review on sustainable design of renewable energy systems, Renewable Sustainable Energy Rev. 16 (2012) 192–207.
[18] R. Khanal, C.W. Lei, A scaling investigation of the laminar convective flow in a solar chimney for natural ventilation, Int. J. Heat Fluid Flow 45 (2014) 98–108.
[19] R. Khanal, C.W. Lei, Solar chimney - a passive strategy for natural ventilation, Energy Build. 43 (2011) 1811–1819.
[20] G.H. Gan, A parametric study of Trombe walls for passive cooling of buildings, Energy Build. 27 (1998) 37–43.
[21] W. Du, Q.R. Yang, J.C. Zhang, A study of the ventilation performance of a series of connected solar chimneys integrated with building, Renewable Energy 36 (2011) 265–271.
[22] H.H. Al-Kayiem, K.V. Sreejaya, S.I.U. Gilani, Mathematical analysis of the influence of the chimney height and collector area on the performance of a roof top solar chimney, Energy Build. 68 (2014) 305–311.
[23] Z.D. Chen, P. Bandopadhayay, J. Halldorsson, C. Byrjalsen, P. Heiselberg, Y. Li, An experimental investigation of a solar chimney model with uniform wall heat flux, Build. Environ. 38 (2003) 893–906.
[24] J. Mathur, S. Mathur, Anupma, Summer-performance of inclined roof solar chimney for natural ventilation, Energy Build. 38 (2006) 1156–1163.
[25] M.M. AboulNaga, S.N. Abdrabboh, Improving night ventilation into low-rise buildings in hot-arid climates exploring a combined wall–roof solar chimney, Renewable Energy 19 (2000) 47–54.
[26] N. Hatami, M. Bahadorinejad, Experimental determination of natural convection heat transfer coefficient in a vertical flat-plate solar air heater, Sol. Energy 82 (2008) 903–910.
[27] M. Yang, P.S. Wang, X.D. Yang, Experimental analysis on thermal performance of a solar air collector with a single pass, Build. Environ. 56 (2012) 361–369.
[28] K.H. Lee, R.K. Strand, Enhancement of natural ventilation in buildings using a thermal chimney, Energy Build. 41 (2009) 615–621.
[29] U. Drori, V. Dubovsky, G. Ziskind, Experimental verification of induced ventilation, J. Environ. Eng. 131 (2005) 820–826.
[30] J.C. DeBlois, M.M. Bilec, L.A. Schaefer, Design and zonal building energy modeling of a roof integrated solar chimney, Renewable Energy 52 (2013) 241–250.

[31] Y.C. Li, S.L. Liu, Experimental study on thermal performance of a solar chimney combined with PCM, Appl. Energy 114 (2014) 172–178.
[32] D.A. Ryan, S. Burek, P. Baker, Experimental investigation into the buoyancy driven convection in passive solar heating facades, in: The 2nd Scottish Conference for Postgraduate Researchers of the Built and Natural Environment, Glasgow Caledonian University, UK, 2005, pp. 683–693.
[33] K.T. Andersen, Theoretical considerations on natural ventilation by thermal buoyancy, ASHRAE Trans. 15 (1995) 81–93.
[34] M. Rahimi, I. Arianmehr, The effect of a vertical vent on single-sided displacement ventilation, ISRN Mech. Eng. 2011 (2011) 1–5.
[35] C. Afonso, A. Oliveira, Solar chimneys: simulation and experiment, Energy Build. 32 (2000) 71–79.
[36] E.P. Sakonidou, T.D. Karapantsios, A.I. Balouktsis, D. Chassapis, Modeling of the optimum tilt of a solar chimney for maximum air flow, Sol. Energy 82 (2008) 80–94.
[37] M. Sandberg, B. Moshfegh, Ventilated-solar roof air flow and heat transfer investigation, Renewable Energy 15 (1998) 287–292.
[38] W.T. Ding, Y. Minegishi, Y. Hasemi, Y. Yamada, Smoke control based on a solar-assisted natural ventilation system, Build. Environ. 39 (2004) 775–782.
[39] W.T. Ding, Y. Hasemi, Smoke control through a double-skin façade used for natural ventilation, ASHRAE Trans. 112 (2006) 181–188.
[40] C.L. Chow, W.K. Chow, Initial buoyancy reduction in exhausting smoke with solar chimney, J. Heat Transfer 132 (2010) 1–3.
[41] M. Hultmark, A.J. Smits, Temperature corrections for constant temperature and constant current hot-wire anemometers, Meas. Sci. Technol. 21 (2010) 105404–105407.
[42] R. Hansen, H. Ingason, Heat release rate measurements of burning mining vehicles in an underground mine, Fire Saf. J. 61 (2013) 12–25.
[43] L. Shi, M.Y.L. Chew, Influence of moisture on autoignition of woods in cone calorimeter, J. Fire Sci. 30 (2012) 158–169.
[44] L. Shi, G.M. Zhang, X.D. Cheng, Y. Guo, J.H. Wang, M.Y.L. Chew, Developing an empirical model for roof solar chimney based on experimental data from various test rig, Build. Environ. 110 (2016) 115–128.
[45] W. Jahn, G. Rein, J.L. Torero, A posteriori modelling of the growth phase of Dalmarnock fire test one, Build. Environ. 46 (2011) 1065–1073.
[46] R. Bryant, C. Womeldorf, E. Johnsson, T. Ohlemiller, Radiative heat flux measurement uncertainty, Fire Mater. 27 (2003) 209–222.
[47] J.H. Wang, G.Q. Li, L. Shi, Y. Jiao, Q.M. Xie, Transport time lag effect on smoke flow characteristics in long-narrow spaces, Fire Technol. 53 (2017) 983–1010.
[48] L. Shi, M.Y.L. Chew, Q.Y. Xie, R.F. Zhang, L.M. Li, C.M. Xu, Experimental study on fire characteristics of PC monitors - part II: full-scale study under different ventilation conditions, J. Appl. Fire Sci. 19 (2010) 41–61.
[49] T.S. Larsen, P. Heiselberg, Single-sided natural ventilation driven by wind pressure and temperature difference, Energy Build. 40 (2008) 1031–1040.
[50] H.J. Wang, Q.Y. Chen, A new empirical model for predicting single-sided, wind–driven natural ventilation in buildings, Energy Build. 54 (2012) 386–394.
[51] R. Bassiouny, N.S.A. Koura, An analytical and numerical study of solar chimney use for room natural ventilation, Energy Build. 40 (2008) 865–873.
[52] L. Shi, G.M. Zhang, An empirical model to predict the performance of typical solar chimneys considering both room and cavity configurations, Build. Environ. 103 (2016) 250–261.
[53] N.K. Bansal, R. Mathur, M.S. Bhandari, Solar chimney for enhanced stack ventilation, Build. Environ. 28 (1993) 373–377.
[54] Y.Z. Yao, X.D. Cheng, S.G. Zhang, K. Zhu, H.P. Zhang, L. Shi, Maximum smoke temperature beneath the ceiling in an enclosed channel with different fire locations, Appl. Therm. Eng. 111 (2017) 30–38.
[55] Y.Z. Li, B. Lei, H. Ingason, The maximum temperature of buoyancy-driven smoke flow beneath the ceiling in tunnel fires, Fire Saf. J. 46 (2011) 204–210.
[56] A.S. Zohrabian, M.R. Mokhtarzadeh-Dehghanb, A.J. Reynoldsb, Buoyancy-driven air flow in a stairwell model with through-flow, Energy Build. 14 (1990) 133–142.
[57] A.S. Zohrabian, M.R. Mokhtarzadeh-Dehghanb, A.J. Reynolds, B.S.T. Marriott, An experimental study of Buoyancy-driven flow in a half-scale stairwell model, Build. Environ. 24 (1989) 141–148.
[58] D.H. Qi, L.Z. Wang, G.C. Zhao, Froude-Stanton modeling of heat and mass transfer in large vertical spaces of high-rise buildings, Int. J. Heat Mass Transfer 115 (2017) 706–716.
[59] A. Andreozzi, N. Bianco, M. Musto, G. Rotondo, Scaled models in the analysis of fire-structure interaction, J. Phys. Conf. Series 655 (2015) 1–9.
[60] Y.A. Cengel, M.A. Boles, Thermodynamics: An Engineering Approach, 8th ed., McGraw-Hill, 2015.
[61] K.S. Ong, C.C. Chow, Performance of a solar chimney, Sol. Energy 74 (2003) 1–17.
[62] J. Mathur, N.K. Bansal, S. Mathur, M. Jain, Anupma, Experimental investigations on solar chimney for room ventilation, Sol. Energy 80 (2006) 927–935.